Alloy Thermal Physical Property Prediction Coupled Computational Thermodynamics with Back Diffusion Consideration

J. Guo and M. T. Samonds

(Submitted October 17, 2006)

Simulation technologies are applied extensively in casting industries to understand the heat transfer and fluid transport phenomena and their relationships to the microstructure and the formation of defects. It is critical to have accurate thermo-physical properties as input for reliable simulations of the complex solidification and solid phase transformation processes. The thermo-physical properties can be calculated with the help of thermodynamic calculations of phase stability at given temperatures and compositions. A multicomponent alloy solidification model, coupled with a Gibbs free energy minimization engine and thermodynamic databases, has been developed. A back diffusion model is integrated so that the solidification conditions, such as cooling rate, can be taken into account.

---

1. Introduction

Solidification proceeds at various rates for castings. Thus the microstructure and the composition are not homogeneous throughout the casting. The solidification path determines the solidification behavior of an alloy. For complex multi-component alloys, the solidification path is very complicated. Hence, the equilibrium of each phase at different temperature needs to be calculated. The thermodynamic and the kinetics calculations are the base for the prediction of solidification. The diffusion transport in the solid phase needs to be solved for each element. This requires knowledge of the diffusion coefficient of the element, the length scale, and the cooling conditions. Thermodynamic modeling has recently become increasingly used to predict the equilibrium and phase relationships in multicomponent alloys.[1,2,3] Currently, several packages are able to simulate

J. Guo and **M. T. Samonds,** ESI US R&D, 5850 Waterloo Road, Suite 140, Columbia, MD 21045. Contact e-mail: jgu@esi-group.com

solidification using the Scheil model and lever rule, such as Thermo-Calc (www.thermocalc.com), Pandat (www.thermocalc.com), and JMatPro (www.thermotech.co.uk). A modified Scheil model is applied in JMatPro. In their calculation, carbon and nitrogen are treated as completely diffused in the solid which makes a great improvement, particularly for iron based alloy solidification. Unfortunately, in all those packages, the finite back diffusion which occurs in reality is not taken into account. In this paper, back diffusion is included in the alloy solidification calculation, with the cooling rate as a user input. The thermodynamic calculation was based on the minimization routines developed by Lukas et al.[1] and extended by Kattner et al.[2]

To obtain the thermo-physical properties experimentally at low temperature can be time consuming and expensive. It becomes even more difficult at high temperatures, especially when it is close to, or above, the solidus temperature. The thermo-physical properties from room temperature to the pouring temperature are all needed in solidification and heat treatment modeling in order to accurately predict the microstructure, defect formation, and mechanical properties of castings or heat treated parts. With the help of thermodynamic calculations, the thermo-physical properties can be predicted.[4,5]

In this paper, first a back diffusion model is presented. The thermo-physical properties model are introduced next. The model can predict density, liquid viscosity, thermal conductivity, and some other properties, which are needed for the modeling of solidification and heat treatment. Some experimental results are presented to validate the models.

2. Back Diffusion Model

Obtaining the solidification path of a commercial alloy is very important for understanding and controlling the solidification process of the alloy. Traditionally there are two ways to predict the alloy solidification path. One is the

complete equilibrium approach, which can be calculated by the lever rule. The other is the Scheil model, which assumes that the solute diffusion in the solid phase is small enough to be considered negligible and that diffusion in the liquid is rapid enough to assume that diffusion is complete. For almost all practical situations, the solidification occurs under non-equilibrium conditions, but does not follow the Scheil model. There is finite diffusion in the solid, or back diffusion, which is a function of the cooling rate.

Segregation due to the solute rejection from the solid during solidification is an active field. Back diffusion plays an important role in the segregation calculation. There are many numerical and analytical models trying to handle such phenomena.[6-12] For most of the models, constant partition coefficients are assumed, which is a good approximation for most of the alloys. Unfortunately, sometimes the partition coefficients can vary dramatically for some commercial alloys. The partition coefficient of an element in an alloy can change from less than one to greater than one, or from greater than one to less than one during solidification.[13] For these cases, the analytical or previous numerical models are invalid. The equilibrium of each phase at different temperatures should be calculated. This can be fulfilled by coupling with the thermodynamic calculation. Recently researchers started to couple thermodynamic calculation with modified Scheil model including back diffusion for solidification simulation.[14]

2.1 Model Equations

In this paper, the liquid is assumed to be completely mixed. The solid concentration is calculated by solving a one-dimensional diffusion equation for each element. Off-diagonal diffusion terms are not included in this analysis. The governing equations for conservation of species for multicomponent alloy solidification are:[15]

Liquid species conservation:

$$f_l \frac{\partial C_l^j}{\partial t} = (C_l^j - C_i^j)\frac{\partial f_s}{\partial t} + \frac{SD_j}{L}(C_s^j - C_i^j) \tag{Eq 1}$$

Solid species conservation:

$$f_s \frac{\partial C_s^j}{\partial t} = (C_i^j - C_s^j)\left(\frac{\partial s}{\partial t} + \frac{SD_j}{L}\right) \tag{Eq 2}$$

where j is the species index, C is concentration, D is a diffusion coefficient, f is the volume fraction of a phase, t is time, L is a diffusion length, and S is the interfacial area concentration. The subscript i refers to the solid-liquid interface, l is the liquid, s is the solid.

The diffusion length L can be determined using a model proposed by Wang and Beckermann[15] based on the work of Ohnaka[16] using the one-dimensional plate-like dendrite geometry, $L = \frac{f_s \lambda}{6}$, where λ is the secondary dendrite arm spacing which is a function of cooling rate, $\lambda = a \dot{T}^n$. Here a and n are constants determined by the alloy composition, and $\dot{T}$ is the cooling rate. The interfacial area concentration S is related to the solid volume fraction and the secondary dendrite arm spacing: $S = \frac{2}{\lambda}$. Combining Eq 1 and 2 and then discretizing, we have:

$$f_s(C_s^j - C_s^{j^o}) = \left(\Delta f_s + \frac{SD\Delta t}{L}\right)C_i^j - \left(\Delta f_s + \frac{SD\Delta t}{L}\right)C_s^j \tag{Eq 3}$$

where the superscript o refers to the old value of the variable. Hence:

$$C_s^j = \frac{(f_s - \Delta f_s)C_s^{j o} + (\Delta f_s + \frac{SD\Delta t}{L})C_i^j}{f_s + \frac{SD\Delta t}{L}} \tag{Eq 4}$$

Equation 4 is used for calculating the concentration in the solid. Here we notice that Eq 4 can automatically turn into the Scheil model or lever rule if the diffusion is zero or infinitely large:

$$C_s^j = C_i^j \text{ when } \frac{SD\Delta t}{L} \to \infty \text{ Lever Rule}$$

$$C_s^j = C_s^{j^o} + (C_i^j - C_s^o)\Delta f_s/f_s \text{ when } \frac{SD\Delta t}{L} = 0 \text{ Scheil model}$$

Based on mass conservation, the liquid concentration can be calculated from the solution of the solid concentration profile accordingly.

2.2 Model Validation

In order to test this model, some calculations were compared with published experimental and numerical results.

2.2.1 Al-4.9% Cu Alloy Solidification. The solidification has been predicted for an aluminum 4.9 percent weight copper alloy at different cooling rates. There will be no eutectic if the lever rule is used. There is about 10% eutectic if the Scheil model is applied. The eutectic amount will be different for different cooling rates. The results are consistent with the experimental measurements as well as other models[5,11] which are shown in Fig. 1. The amount of eutectic can be well predicted with the current model.
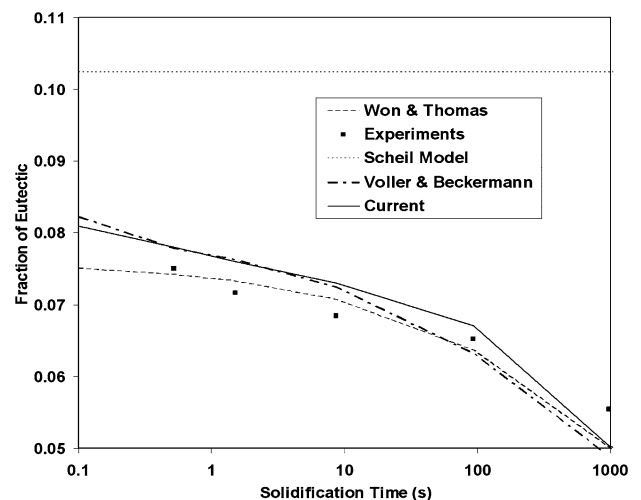

Fig. 1 Eutectic fraction of Al-4.9% Cu alloy with different solidification times
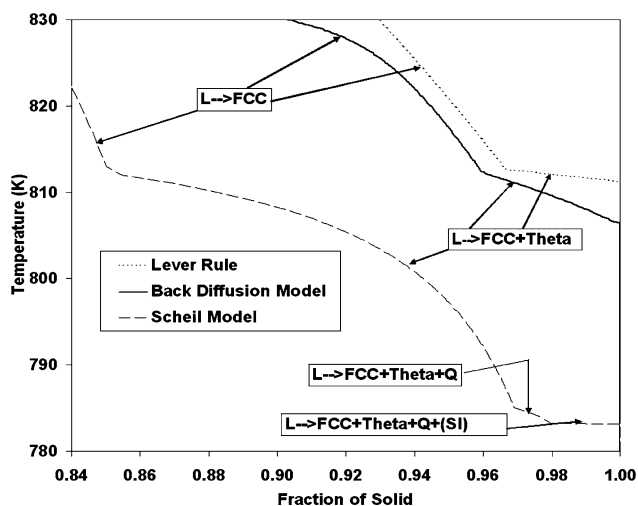
Fig. 2 Solidification path of a 2219 Al alloy

2.2.2 2219 Al-Cu-Mg Alloy Solidification. Yan[14] did an experiment for the solidification of a quaternary Al-6.27Cu-0.22Si-0.19Mg alloy, with a cooling rate of 0.065 K/s. The microstructure of the solidified samples is dendritic. The calculated fraction of solid versus temperature relationship for this quaternary alloy with a cooling rate of 0.065 K/s is shown in Fig. 2. According to the Scheil model, the solidification sequence for this alloy is: L → L + fcc → L + fcc + Theta → L + fcc + Theta + $Al_5Cu_2Mg_8Si_6$(Q) → L + fcc + Theta + $Al_5Cu_2Mg_8Si_6$ (Q) + Si. Experimentally, there were no Si and $Al_5Cu_2Mg_8Si_6$ phases formed according to metallographical examination and EPMA analysis. The current back diffusion model indicates that there are only fcc and Theta phases formed during solidification for this cooling condition. The results predicted by the back diffusion mode are in agreement with the experimental quantitative image analysis program.

The measured fractions of fcc phase were compared with the calculations from the Scheil model, lever rule, and the current back diffusion model for three different cooling rates. The comparison is shown in Table 1.

The fraction of fcc phase calculated from the Scheil model is less than the measured values and the fraction of fcc calculated from lever rule is higher than that from the experiments for all three cooling rates. The back diffusion model, which takes into account the cooling rate gives good agreement with the experiments.

Table 1   Comparison of experimental and calculated fraction of fcc phase (vol.%)

Cooling rate, K/s	Area scan	Image analysis	Calculation
Lever rule	...	...	96.7
0.065	96.0	95.4	96.0
0.25	95.8	95.3	95.4
0.75	95.8	94.7	94.3
Scheil model	...	...	85.4

2.2.3 Solidification Ending Temperature Prediction. The liquidus temperatures will be the same based on the lever rule and Scheil model calculations. On the other hand, the solidification ending temperature could be very different. Hence, the solidification intervals are very different from the calculation based on different models. In the modeling of casting and solidification, the solidification intervals are one of the most important parameters. It dramatically affects the calculated defect formation, such as porosity, hot tearing, and microstructure. For this reason, it is critical to have an accurate solidification ending temperature which corresponds to the real casting process. The cooling rate should be included in such a prediction. For a fixed composition alloy, the cooling rate will be different if different casting technologies are applied; for instance, sand casting or die casting. The cooling rate will be different even for the same casting but at different locations. The solidification ending temperature is almost always different from the value calculated from the lever rule or Scheil model. The difference is determined by the cooling history. Figure 3 shows the comparison between experimental and calculated solidification ending temperature for different alloys with the Scheil model, lever rule, and current back diffusion model. For the back diffusion calculation, the cooling rates were based on the experimental conditions if they are available. Otherwise, some approximated cooling rates were used, such as 1,000 K/s for die casting and 10 K/s for sand casting. It tells us that the calculated solidification ending temperatures are higher than the experimental ones if the lever rule is applied. Sometimes the difference can be as high as several hundred degrees for some alloys. On the other side, the Scheil model calculation gives lower values of the solidification ending temperature than that from the experiments. The back diffusion calculations give an excellent result for solidification ending temperature compared with that from the experiments.
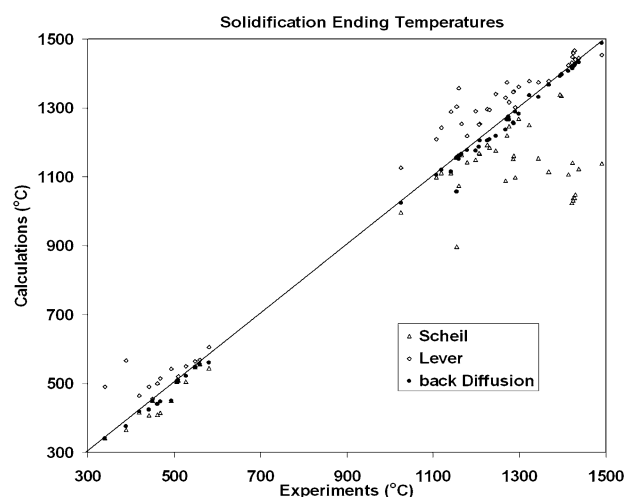

Fig. 3 Comparison between experimental and calculated solidification ending temperature for different alloys with Scheil model, lever rule, and back diffusion model

3. Thermo-Physical Properties Calculation

The research on thermo-physical properties is a very important part of materials science, particularly at the current time because such data is a critical input for the simulation of metals processing. Lee and coworkers investigated the sensitivity of investment casting simulations to the accuracy of thermo-physical properties.[17] They found that the temperature prediction and thermal gradient in the liquid are the most sensitive to the accuracy of the input values used for density and thermal conductivity in the solid. Thermal conductivity in the liquid, specific heat, and density have similar levels of influence on solidification time; increasing their values increases the local solidification time. Thermal conductivity in the solid has the opposite effect compared to all the other properties studied.

Accurate thermo-physical data are experimentally difficult to obtain at high temperatures, especially for reactive alloys such as titanium and nickel-based superalloys. An extensive database for the calculation of thermo-physical properties has been developed which utilizes the phase fraction information predicted with the Gibb's free energy minimization routines developed by Lukas et al.[1] and extended by Kattner et al.[2] These properties include density, specific heat, enthalpy, latent heat, electrical conductivity and resistivity, thermal conductivity, liquid viscosity, Young's modulus, and Poisson's ratio. The thermodynamic calculation is based on the thermodynamic databases from CompuTherm LLC (Madison, WI 53719, USA). All the following experiments were based on a cooling rate of 20 K/min. Hence, the same cooling was used for back diffusion calculation.

A simple pair-wise mixture model, which is similar to that used to model thermodynamic excess functions in multicomponent alloys, is used to calculate the properties.[3]

$$P = \sum x_i P_i + \sum_i \sum_{j \geq i} x_i x_j \sum_v \Omega_v (x_i - x_j)^v \qquad \text{(Eq 5)}$$

where P is the phase property, P_i is the property of the pure element in the phase, Ω_i is a binary interaction parameter, and x_i and x_j are the mole fractions of elements i and j in that phase.

3.1 Thermal Conductivity

The thermal conductivity mainly depends on the chemical composition of an alloy. It also depends to a lesser extent on the precipitates, bulk deformation, microstructures, and other factors.[18,19] These factors can usually be ignored in the calculation of conductivity for commercial alloys.

The thermal conductivity of alloys is composed of two components: a lattice component and an electronic component. In well conducting metals, the thermal conductivity is mainly electronic conductivity. The lattice conductivity is usually very small compared to the electronic one. Hence, we only consider the electronic component here. The thermal conductivity λ and the electrical resistivity ρ are related according to the Wiedeman-Franz-Lorenz law.[19,20,21]

$$\lambda = \frac{LT}{\rho} \qquad \text{(Eq 6)}$$

where the Lorentz constant $L = 2.44 \times 10^{-11} W\Omega K^{-2}$, T is the temperature.

An example of the calculated thermal conductivity of an A356 alloy is shown in Fig. 4 with experimental results for comparison. The calculation can accurately predict the thermal conductivity variation with temperatures for this alloy in the liquid, solid, and mushy zone. Figure 5 shows the comparison with experimental results from Auburn University for various alloys at different temperatures (http://metalcasting.auburn.edu/data/data.html). The agreement is good in general.

3.2 Liquid Viscosity

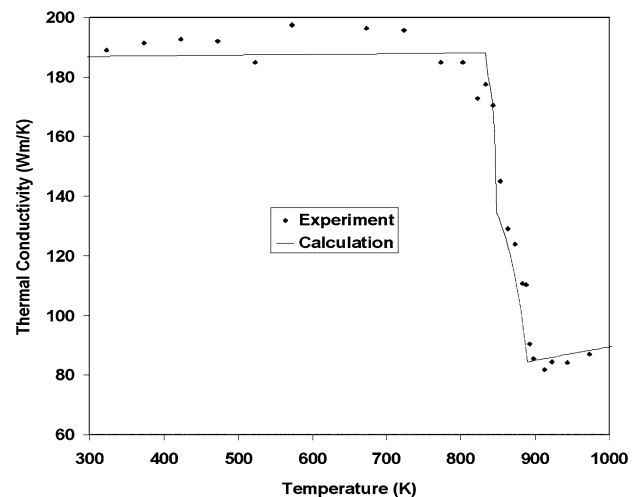Viscosity is an important property to be considered in dealing with fluid flow behavior and in understanding the

Fig. 4 Comparison between experimental and calculated thermal conductivity for an A356 alloy
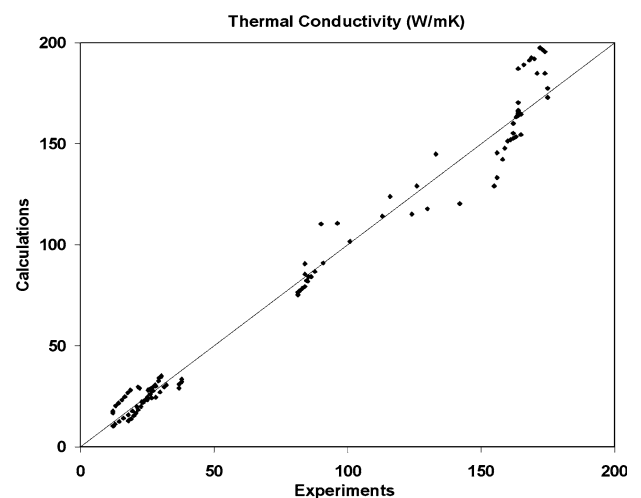

Fig. 5 Comparison between experimental and calculated thermal conductivity for different alloys

kinetics of reactions of relevance to process metallurgy. The liquid viscosity is a measure of resistance of the fluid to flow when subjected to an external force. There are two approaches to modeling of complex alloy viscosity. One is the fundamental molecular approach and the other is the semi-theoretical procedure. The former one is mainly based on the monatomic nature. There are some models available, but most of them are still under development and don't meet the technological need. The semi-theoretical method is applied in this paper to predict the viscosity of alloys. The viscosity η of pure liquid metals follows Andrade's relationship:[22]

$$\eta(T) = \eta_o \exp(E/RT) \qquad (\text{Eq } 7)$$

where E is the activation energy, R is the gas constant.

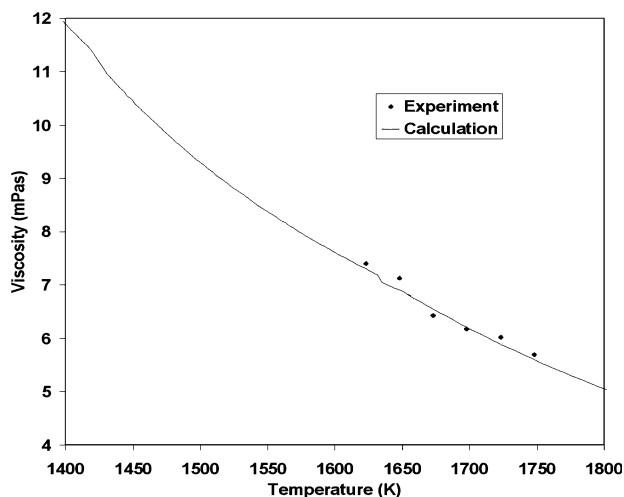Figure 6 shows an example of the calculated liquid viscosity of an IN718 alloy using the mixture model compared with experimental results. Figure 7 shows the comparison between experimental and calculated results for various alloys at different temperatures.

3.3 Density

Currently the mathematical models have now reached the stage where one of the limiting factors in their applicability is the accuracy of the thermo-physical data for the materials to be modeled. Among all the thermo-physical data, the temperature dependent density is critical for the accurate simulation of solidification microstructure and defect formation.[17] A database has been developed containing molar volume and thermal volume coefficients of expansion of liquid, solid solution elements, and intermetallic phases. This is linked to the thermodynamic calculations mentioned above. The densities of the liquid and solid phases of multicomponent systems are calculated by the simple mixture model.[23] Figure 8 shows plots comparing experimental values with calculations for the density of different alloys at different temperatures. Figure 9 shows a comparison between the calculated and experimentally reported density for a CF8M stainless steel alloy.

It can be concluded that the current model is able to calculate the thermo-physical properties of multicomponent alloys accurately in the liquid, mushy zone, and solid, thanks to the thermodynamic calculations and back diffusion model.

4. Conclusions

A multicomponent alloy solidification model, which is coupled with thermodynamic calculations, has been developed. The finite back diffusion is included to take into account the different cooling rates for different casting processes. The thermo-physical properties, such as density, thermal conductivity, and liquid viscosity, can be calculated accurately for dependable solidification and heat treatment

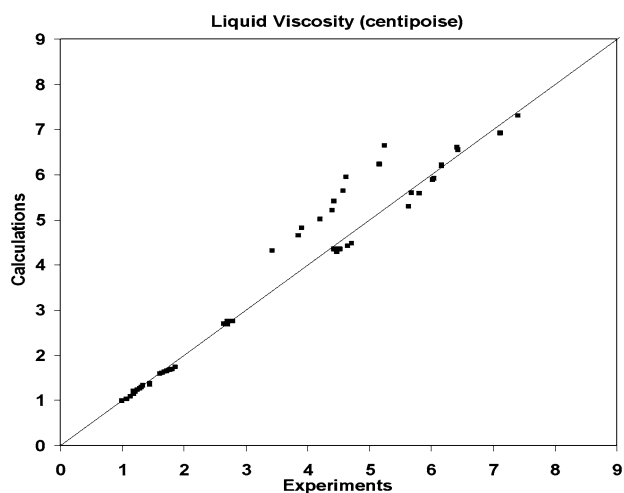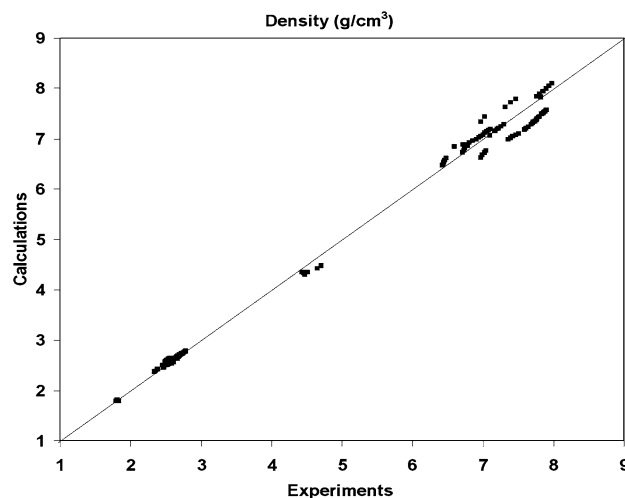**Fig. 6** Comparison between experimental and calculated viscosity for an IN718 alloy

Fig. 7 Comparison between experimental and calculated viscosity for different alloys

Fig. 8 Comparison between experimental and calculated density for different alloys
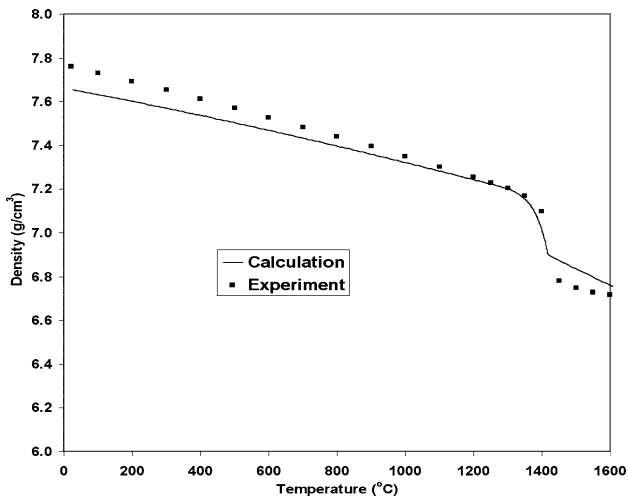
Fig. 9 Comparison between experimental and calculated density for a CF8M Stainless Steel

simulation. The model has been validated on different alloys.

References

1. H.L. Lukas, J. Weiss, and E.Th. Henig, Strategies for the Calculation of Phase Diagrams, *CALPHAD*, 1982, **6**(3), p 229-251
2. U.R. Kattner, The Thermodynamic Modeling of Multicomponent Phase Equilibria, *JOM*, 1997, **49**, p 14-19
3. N. Saunders and A.P. Miodownik, *CALPHAD: Calculation of Phase Diagrams A Comprehensive Guide*. Elsevier Science Ltd, New York, NY, 1998 299-411
4. N. Saunders, Z. Guo, X. Li, A.P. Miodownik, and J-Ph. Schillé, Using JMatPro to Model Materials Properties and Behavior, *JOM*, 2003, **Dec**., p 65
5. J. Guo and M.T. Samonds, Property Prediction With Coupled Macro-Micromodeling and Computational Thermodynamics, Hwang Weng-Sing and Kaohsiung, Ed., *Modeling of Casting & Solidification Processes*, Taiwan, 2004, p 157-164
6. H.D. Brody and M.C. Flemings, Solute Redistribution during Dendrite Solidification, *Trans. Met. Soc. AIME*, 1966, **236**, p 615
7. T.W. Clyne and W. Kurz, Solute Redistribution during Solidification with Rapid Solid State Diffusion, *Metall. Trans.*, 1981, **12A**, p 965
8. I. Ohnaka, Mathematical Analysis of Solute Redistribution during Solidification with Diffusion in Solid Phase, *Trans. ISIJ*, 1986, **26**, p 1045
9. C.Y. Wang and C. Beckermann, Unified Solute Diffusion Model for Columnar and Equiaxed Dendritic Alloy Solidification, *Mater. Sci. Eng.*, 1993, **171**, p 199
10. L. Nastac and D.M. Stefanescu, An Analytical Model for Solute Redistribution during Solidification of Plannar, Columnar and Equiaxed Morphology, *Metall. Trans.*, 1993, **24**, p 2107
11. V.R. Voller and C. Beckermann, A Unified Model of Microsegregation and Coarsening, *Metall. Trans.*, 1999, **30**, p 2183
12. V.R. Voller, On a General Back-diffusion Parameter, *J. Cryst. Growth*, 2001, **226**, p 562-568
13. M.C. Schneider, J.P. Gu, C. Beckermann, W.J. Boettinger, and U.R. Kattner, Modeling of Micro- and Macrosegregation and Freckle Formation in Single-Crystal Nickel-Base Superalloy Directional Solidification, *Met. Mat. Trans. A*, 1997, **28A**, p 1517-1531
14. X. Yan, Thermodynamic and Solidification Modeling Coupled with Experimental Investigation of the Multicompoent Aluminum Alloys, Ph.D. Thesis, University of Wisconsin-Madison, Madison, WI, 2001
15. C.Y. Wang and C. Beckermann, A Multiphase Solute Diffusion Model for Dendritic Alloy Solidification, *Met. Trans. A*, 1993, **24A**, p 2787-2802
16. I. Ohnaka, Mathematical Analysis of Solute Redistribution during Solidification with Diffusion in Solid Phase, *Trans. ISIJ*, 1986, **26**, p 1045-1052
17. X.L. Yang, P.D. Lee, R.F. Brooks, and R. Wunderlich, The Sensitivity of Investment Casting Simulations to the Accuracy of Thermophysical Property Values, TMS Ed., *Superalloys*, The Minerals, Metals & Materials Society, 2004
18. B. Alkan, R. Karabulut, and B. Unal, Electrical Resistivity of Liquid Metals and Alloys, *Acta Phys. Pol. A,*, 2002, **102**, p 385-400
19. P.L. Rossiter, *The Electrical Resistivity of Metals and Alloys*. Cambridge University Press, New York, NY, 1987 137-272
20. A. Rudajevova, M. Stanek, and P. Lukac, Determination of Thermal Diffusivity and Thermal Conductivity of Mg-Al Alloys, *Mat. Sci. Eng., A*, 2003, **A341**, p 152-157
21. P.G. Klemens and R.K. Williams, Thermal Conductivity of Metals and Alloys, *Int. Mat. Rev.*, 1986, **31**(5), p 197-215
22. D. Sichen, J. Bygden, and S. Seetharaman, A Model for Estimation of Viscosities of Complex Metallic and Ionic Melts, *Met. Mat. Trans. B*, 1994, **25B**, p 519-525, August
23. N. Saunders, X. Li, A.P. Miodownik, and J.P. Schille, Modeling of the Thermo-Physical and Physical Properties for Solidification of Al-Alloys, *Light Metals*, 2003, p 999–1004